Journal of Neurochemistry

JOURNAL OF NEUROCHEMISTRY | 2010 | 113 | 1252–1262 doi: 10.1111/j.1471-4159.2010.06692.x

Despite its role in assembly, methionine 35 is not necessary for amyloid β-protein toxicity

Panchanan Maiti,* Aleksey Lomakin,† George B. Benedek†,‡ and Gal Bitan*,§,¶

*Department of Neurology, David Geffen School of Medicine, University of California, Los Angeles, California, USA
†Materials Processing Center, Massachusetts Institute of Technology, Cambridge, Massachusetts, USA
‡Department of Physics, Massachusetts Institute of Technology, Cambridge, Massachusetts, USA
§Brain Research Institute, University of California, Los Angeles, California, USA
¶Molecular Biology Institute, University of California, Los Angeles, California, USA

Abstract

An important component of the pathologic process underlying Alzheimer's disease is oxidative stress. Met^{35} in amyloid β-protein (Aβ) is prone to participating in redox reactions promoting oxidative stress, and therefore is believed to contribute significantly Aβ-induced toxicity. Thus, substitution of Met^{35} by residues that do not participate in redox chemistry would be expected to decrease Aβ toxicity. Indeed, substitution of Met^{35} by norleucine (Nle) was reported to reduce Aβ toxicity. Surprisingly, however, substitution of Met^{35} by Val was reported to increase toxicity. Aβ toxicity is known to be strongly related to its self-assembly. However, neither substitution is predicted to affect Aβ assembly substantially. Thus, the effect of these substitutions on toxicity is difficult to explain. We revisited this issue and compared Aβ40 and Aβ42 with analogs containing $Met^{35} \rightarrow$ Nle or $Met^{35} \rightarrow$ Val substitutions using multiple biophysical and toxicity assays. We found that substitution of Met^{35} by Nle or Val had moderate effects on Aβ assembly. Surprisingly, despite these effects, neither substitution changed Aβ neurotoxicity significantly in three different assays. These results suggest that the presence of Met^{35} in Aβ is not important for Aβ toxicity, challenging to the prevailing paradigm, which suggests that redox reactions involving Met^{35} contribute substantially to Aβ-induced toxicity.

Keywords: Alzheimer's disease, amyloid β-protein, oxidative stress, neurotoxicity, structure–activity relationship.
J. Neurochem. (2010) **113**, 1252–1262.

Alzheimer's disease (AD) is a progressive, age-related neurodegenerative disorder, which gradually impairs cognitive abilities, causes difficulties in execution of routine tasks, and finally leads to dementia and death (Selkoe 2001; Cummings 2004). Amyloid plaques, neurofibrillary tangles, neurite dystrophy, synapse loss, and neurodegeneration in the cerebral cortex and hippocampus are pathologic hallmarks of AD (Selkoe 2001). Genetic, physiologic, and biochemical data indicate that self-assembly of amyloid β-protein (Aβ) initiates the disruption of interneuronal communication in AD (Roher *et al.* 1993; Hardy and Selkoe 2002; Roychaudhuri *et al.* 2009). Though initially Aβ fibrils, the pre-dominant component of amyloid plaques, were thought to be the culprit, now soluble Aβ oligomers are believed to be the major neurotoxic species in AD (Dahlgren *et al.* 2002; White *et al.* 2005; Haass and Selkoe 2007; Tomic *et al.* 2009). Plaque formation is thought to be an attempt of the brain to sequester the toxic oligomers in a less harmful fibrillar structure (Bravo *et al.* 2008; Josephs *et al.* 2008; Reiman *et al.* 2009), though plaques also may serve as reservoirs of oligomeric Aβ (Koffie *et al.* 2009).

Received December 14, 2009; revised manuscript received March 9, 2010; accepted March 15, 2010.

Address correspondence and reprint requests to Gal Bitan, PhD, Department of Neurology, Room 451, Neuroscience Research Building 1, Charles E. Young Drive South, Los Angeles, CA 90095, USA. E-mail: gbitan@mednet.ucla.edu

Abbreviations used: AD, Alzheimer's disease; Aβ, amyloid β-protein; CD, circular dichroism spectroscopy; DLS, dynamic light scattering; EM, electron microscopy; HFIP, 1,1,1,3,3,3-hexafluoroisopropanol; LDH, lactate dehydrogenase; MTT, 3-(4,5-dimethylthiazol-2-yl)-2,5-diphenyltetrazolium bromide; PICUP, photo-induced cross-linking of unmodified proteins; ROS, reactive oxygen species; SDS–PAGE, sodium dodecyl sulfate–polyacrylamide gel electrophoresis; TUNEL, terminal deoxyribonucleotidyl transferase dUTP nick end labeling; WT, wild-type.

The C-terminal region of Aβ plays a key role in controlling Aβ oligomerization and aggregation (Jarrett *et al.* 1993; Bitan *et al.* 2003a,c). Within this region, oxidation of Met^{35} to sulfoxide has been reported to alter substantially Aβ oligomerization (Hou *et al.* 2002, 2004; Palmblad *et al.* 2002; Bitan *et al.* 2003b) and neurotoxicity (Varadarajan *et al.* 1999, 2000, 2001; Barnham *et al.* 2003; Ciccotosto *et al.* 2004). The sulfoxide form of Aβ has been found in cerebral tissue extracts derived from patients with AD and transgenic mice (Näslund *et al.* 1994; Kuo *et al.* 2001). Whether these findings point to a causative effect of oxidation of Aβ to the sulfoxide in AD or are merely a result of the oxidative environment in the AD brain, or a protein-extraction-induced artifact, is an open question.

Redox reactions in the AD brain generate highly reactive free radicals (Butterfield 2002; Halliwell 2006). To regain stability, these radicals abstract electrons or hydrogen atoms from neighboring molecules or groups, leading to perturbation of the chemical structure, and destruction of biologic molecules (Butterfield *et al.* 2007). Free radicals normally form in a controlled manner in the mitochondrial respiratory chain during oxidative phosphorylation when molecular oxygen is reduced to water (Halliwell 2006). During this process, two reactive oxygen species (ROS) form: superoxide anion (O_2^-) and hydrogen peroxide (H_2O_2). In addition, O_2^- or H_2O_2 may be generated by multiple other enzymatic and non-enzymatic cellular mechanisms (Halliwell 1989). H_2O_2 may further form hydroxyl radicals *via* Fenton chemistry (Markesbery and Lovell 1998; Halliwell 2006). When the control mechanisms that maintain these and other ROS are compromised, as happens in AD, the result is oxidative damage, including lipid peroxidation, protein carbonylation, and other modifications of essential biomolecules (Markesbery and Lovell 1998; Halliwell 2006; Butterfield *et al.* 2007; Crouch *et al.* 2008).

Under the highly oxidative environment in the AD brain, oxidation of Met^{35} in Aβ may lead to formation of Met-sulfuranyl radicals, which may initiate, or participate in, the destructive chemistry described above. Thus, oxidation of Met^{35} in Aβ has been postulated to be directly involved in Aβ toxicity. Alternatively, neurotoxic mechanisms caused by Aβ oligomers, including disruption of Ca^{2+} homeostasis and excitotoxicity (Piacentini *et al.* 2008), may cause oxidative stress that would, among other things, oxidize Met^{35} in Aβ, as a result, not cause, of Aβ toxicity.

If Met^{35} oxidation causes Aβ toxicity, substitution of Met^{35} by aliphatic residues that lack sulfur, do not form radicals easily, and are not substrate for ROS, would be expected to suppress Aβ toxicity. In line with this hypothesis, substitution of Met^{35} by Nle has been reported to decrease Aβ toxicity (Varadarajan *et al.* 1999; Yatin *et al.* 1999; Butterfield and Kanski 2002; Clementi *et al.* 2006). Surprisingly, however, substitution of Met^{35} by Val had the opposite effect (Ciccotosto *et al.* 2004). Complicating matters further, Ciccotosto *et al.* reported that [Val^{35}]Aβ42 produces similar amounts of H_2O_2 as Aβ42, whereas Murray *et al.* found that [Val^{35}]Aβ42 showed reduced lipid peroxidation relative to Aβ42 (Murray *et al.* 2005).

Because Met^{35} resides in the middle of the hydrophobic C-terminus of Aβ, and because Met, Nle, and Val all are hydrophobic residues, the $Met^{35} \rightarrow$ Nle or $Met^{35} \rightarrow$ Val substitutions are not expected to have a strong effect on Aβ assembly. Indeed, substitution of Met^{35} by Nle had little effect on the oligomer size distribution of Aβ (Bitan *et al.* 2003b).

Because substantial efforts have been dedicated to understanding the role of Met^{35} in Aβ in AD, we felt that the discrepancy between previous studies using similar strategies to answer the same question merited a re-examination. Here, we addressed this discrepancy by investigating the effect of substituting Met^{35} in Aβ40 and Aβ42 by either Nle or Val. We describe a systematic, side-by-side comparison of each substituted Aβ analog using assays for oligomer size distribution, conformational change, assembly size, fibril morphology, and toxicity in primary neurons.

Materials and methods

Chemicals and supplies

Silver-staining kit, 10–20% gradient Tris-tricine gels, penicillin/streptomycin, and APO-5-bromo-2-deoxyuridine (BrdU) apoptosis detection kit were purchased from Invitrogen (Carlsbad, CA, USA). Tris(2,2′-bipyridyl)ruthenium dichloride, ammonium persulfate, glutaraldehyde, uranyl acetate, cytosine arabinofuranoside, and poly D-lysine were from Sigma (St. Louis, MO, USA). 1,1,1,3,3,3-Hexafluoroisopropanol (HFIP) was from TCI America (Portland, OR, USA). Trypsin-EDTA solution, Dulbecco's Modified Eagle's Medium, Leibovitz's L-15 medium, and fetal bovine serum were from ATCC (Manassas, VA, USA). Electron microscopy (EM) grids were purchased from Electron Microscopy Science (Hatfield, PA, USA). Cover slips and 96-well black and white plates were from Fisher scientific (Tustin, CA, USA). CytoTox-ONE™ Homogeneous Membrane Integrity Assay kits and 2,5-diphenyltetrazolium bromide were from Promega (Madison, WI, USA).

Animals

All experiments were performed in accordance with the National Research Council Guide for the Care and Use of Laboratory Animals and were approved by the UCLA Institutional Animal Care Use Committee. Pregnant, E18, Sprague-Dawley rats were purchased from Charles River laboratory (Wilmington, MA, USA).

Peptides synthesis

Aβ40, [Nle^{35}]Aβ40, [Val^{35}]Aβ40, Aβ42, [Nle^{35}]Aβ42, and [Val^{35}]Aβ42 were synthesized, purified and characterized by the UCLA Biopolymers Laboratory as described previously (Lomakin *et al.* 1996). Briefly, peptides were synthesized on an automated peptide synthesizer (Model 433A, Applied Biosystems, Foster City, CA, USA) using 9-fluorenylmethoxycarbonyl chemistry and purified by reverse-phase HPLC. Quantitative amino acid analysis and mass spectrometry were used to characterize the expected compositions and molecular masses, respectively, for each peptide.

Preparation of peptide solutions

Purified peptides were stored as lyophilized powders at −20°C. Before use, peptides were treated with HFIP and stored as dry films at −20°C as described previously (Rahimi *et al.* 2009). For biophysical measurements, immediately before use, films were dissolved in 60 mM NaOH at 10% of the desired volume. The solution then was diluted to 50% of the desired volume with deionized water (18.2 MΩ produced by a Milli-Q system, Millipore, Bedford, MA, USA) and sonicated for 1 min. Then, the solution was diluted with 20 mM sodium phosphate, pH 7.4, to the final peptide concentration, which was 10 μM unless stated otherwise. For toxicity experiments, peptides were diluted with cell-culture media after initial dissolution in 10% NaOH, and then sonicated for 1 min.

Photo-cross-linking and SDS–PAGE analysis

The experimental protocol was described previously (Vollers *et al.* 2005; Bitan 2006; Rahimi *et al.* 2009). Briefly, peptide solutions were centrifuged at 14 000 *g* for 10 min. The supernates were subjected to photo-induced cross-linking of unmodified proteins (PICUP) (Fancy and Kodadek 1999). For each cross-linking reaction, 2 μL of 1 mM tris(2,2′-bipyridyl)ruthenium dichloride and 2 μL of 20 mM ammonium persulfate were added to 18 μL of peptide solution. The mixtures were irradiated with visible light for 1 s and the reaction was quenched immediately with 10 μL of Tricine sample buffer (Invitrogen) containing 5% β-mercaptoethanol. The cross-linked peptides were boiled for 5 min and analyzed by sodium dodecyl sulfate–polyacrylamide gel electrophoresis (SDS–PAGE), silver stained, and subjected to densitometric analysis using Image J (NIH software, http://rsb.info.nih.gov). The data are an average of six independent experiments.

Circular dichroism spectroscopy (CD)

Samples were incubated at 25°C with continuous agitation using an orbital shaker at 200 rpm. Spectra were recorded every 2 h during the first 12 h, and then at 24, 48, and 72 h, using a J-810 spectropolarimeter (Jasco, Easton, MD, USA) equipped with a thermostable sample cell at 25°C using 1-mm path-length cuvettes. Spectra were collected from 190 to 260 nm with 1-s response time, 50-nm/min scan speed, 0.2-nm resolution and 2-nm bandwidth, and averaged after background subtraction. The data are representative of three independent experiments.

Dynamic light scattering (DLS)

Samples were prepared as described above, filtered immediately before the first measurement through 20-nm cutoff, Anotop filters (Whatman, Florham Park, NJ, USA), and incubated at 22°C without agitation. Measurements were performed using an in-house-built system with a He-Ne laser model 127 (wavelength 633 nm, power 60 mW, Spectra Physics lasers, Mountain View, CA, USA). Light scattered at 90° was collected using image transfer optics and detected by an avalanche photodiode built into a PD4047 multitau correlator (Precision Detectors, Bellingham, MA, USA). The size distribution of scattering particles was reconstructed from the correlation function of the scattered light using PrecisionDeconvolve (Precision Detectors) based on the regularization method by Tikhonov and Arsenin (Tikhonov, 1977). The data are representative of two independent experiments.

Electron microscopy (EM)

Samples were incubated at 25°C with continuous agitation using an orbital shaker at 200 rpm. Eight-μL aliquots were applied to glow-discharged, carbon-coated Formvar grids for 20 min. The solution was wicked gently with filter paper. Then the samples were fixed with 5 μL of 2.5% glutaraldehyde for 4 min and stained with 5 μL of 1% uranyl acetate for 3 min. The solution was wicked off and the grids were air-dried. The morphology was visualized using a CM120 (FEI, Philips, Hillsboro, OR, USA) transmission electron microscope.

Cell culture

Primary neurons were prepared from E18 rat embryos as described previously (Segal and Manor 1992). Briefly, E18 pregnant rats were killed with CO_2 and the pups were collected immediately. The brains were dissected in chilled Leibovitz's L15 medium in the presence of penicillin/streptomycin (1 μg/mL). The tissue was incubated with 0.25% trypsin-EDTA solution for 30 min and then mechanically dissociated in a small volume of Leibovitz's L15 media using a fire-polished Pasteur pipette. The cells were suspended in Dulbecco's Modified Eagle's Medium containing 10% heat-inactivated fetal bovine serum and penicillin/streptomycin (1 μg/mL), and plated in poly D-lysine (0.1 mg%)-coated 96-well plates (COSTAR, Corning, Lowell, MA, USA) at a density of 3×10^5 cells/mL. The cultures were maintained at 37°C in a humidified atmosphere of 5% CO_2 for 6 days before treatment with peptides. Twenty-four hours after plating, the medium was replaced with fresh medium supplemented with 5 μM cytosine β-D-arabinofuranoside to inhibit the proliferation of glial cells.

MTT assay

Cells were treated with freshly prepared Aβ analogs for 48 h. Cell viability was measured using the 3-(4,5-dimethylthiazol-2-yl)-2,5-diphenyltetrazolium bromide (MTT) cell-metabolism assay, as described previously (Fradinger *et al.* 2008). Briefly, following treatment, 15 μL of MTT were added to each well and incubated for 4 h at 37°C. Then, stop solution was added and kept overnight at 25°C. The optical density was measured using a Synergy plate reader (Bio-TEK instruments, Winooski, VT, USA). The cell viability results of three independent experiments (6 wells per condition) were normalized to the medium control group and expressed as mean ± SEM.

Lactate dehydrogenase (LDH) assay

Neurons were incubated with freshly prepared Aβ analogs for 48 h and cell death was assayed by measuring the release of LDH using CytoTox-ONE™ Homogeneous Membrane Integrity Assay kit (Promega) according to the manufacturer's instructions. Data from three independent experiments (6 wells per condition) were normalized to medium control and expressed as mean ± SEM.

TUNEL assay

Neurons were grown on poly D-lysine-coated cover slips and treated with freshly prepared Aβ analogs for 48 h. The cells were then washed with phosphate-buffered saline and fixed with 4% paraformaldehyde. Cover slips then were treated with ethanol for 30 min at −20°C, followed by 3 × 5 min washes with the 'wash buffer' supplied in the kit, and incubated with terminal deoxynucleotidyl

transferase dUTP nick end labeling (TUNEL) DNA labeling solution for 1 h at 37°C. The cells were washed and treated with an anti-BrdU antibody for 30 min at 25°C in the dark. Cover slips then were washed with the 'rinse buffer' supplied in the kit and counter-stained with 1% propidium iodide for 15 min in the dark, washed with deionized water, dehydrated, cleared, and mounted on glass slides using glycerol. Fluorescent signals were visualized using a Nikon Eclipse E400 microscope (Nikon Instruments Inc., Melville, NY, USA) at λ_{ex} = 480 nm and λ_{em} = 530 nm. Images were merged using the bundled software 'Picture Frame' (Optronics, Goleta, CA, USA). Images were taken from multiple fields in at least three independent experiments and the number of TUNEL-positive cells divided by the total number of counted cells was expressed as percentage apoptotic death (mean ± SEM).

Data analysis

Data were analyzed using a one-way ANOVA with Tukey's pair-wise comparison test as a *post hoc* test using Prism 5.0b (GraphPad, La Jolla, CA, USA).

Results

Effect of substitution of Met^{35} by Nle or Val on Aβ oligomerization

A possible explanation of the different effects of substitution of Met^{35} by Nle or Val on Aβ toxicity is that the substitutions have a profound effect on Aβ assembly. Though this would be unexpected given the similar hydrophobic nature of all three-side chains, we felt that it was an important hypothesis to examine.

To test the effect of substituting Met^{35} by Nle or Val on the oligomer size distribution of Aβ, the wild-type (WT) and substituted Aβ40 and Aβ42 analogs each were cross-linked using PICUP, fractionated by SDS–PAGE and silver-stained (Fig. 1a). Uncross-linked WT and substituted analogs of Aβ40 migrated as monomers, whereas Aβ42 analogs migrated as a combination of monomer and a broad and smeary trimer/tetramer band (data not shown) as described previously (Bitan *et al.* 2003a,b,c). Substitution of Met^{35} by Nle or Val in Aβ40 had little effect on the oligomer size distributions obtained using PICUP (Fig. 1a and b). All three peptides had comparable abundance of monomer through trimer, followed by a lower abundance of tetramer (Fig. 1a), similar to data reported previously (Bitan *et al.* 2001, 2003a).

Aβ42 analogs showed high abundance of pentameric and hexameric paranuclei as described previously (Bitan *et al.* 2003a) (Fig. 1a). Substitution of Met^{35} by Nle or Val yielded lower abundance of dimer and trimer and higher abundance of tetramer, pentamer, and hexamer (Fig. 1a and c). These differences, particularly the decrease in dimer and increase in tetramer abundance, were subtle for [Nle^{35}]Aβ42 and more pronounced for [Val^{35}]Aβ42. Statistical analysis of densitometric data showed that the differences between WT Aβ42

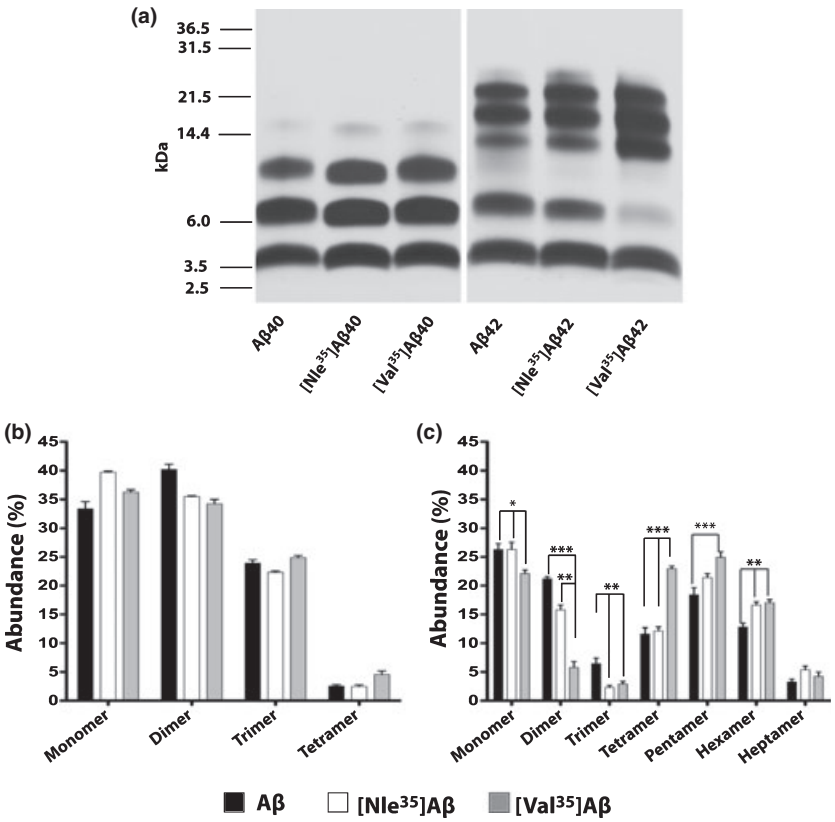

Fig. 1 Oligomer size distribution of amyloid β-protein (Aβ) analogs. Peptides were cross-linked using photo-induced cross-linking of unmodified proteins immediately after preparation, fractionated by sodium dodecyl sulfate–polyacrylamide gel electrophoresis, and the gels silver-stained. (a) A representative gel showing the oligomer size distribution of each analog. The migration of molecular weight markers is shown on the left. (b) Relative band abundance of cross-linked Aβ40 analogs. (c) Relative band abundance of cross-linked Aβ42 analogs. The relative abundance of each band was calculated as a percentage of the entire lane. The data in panels b and c are an average of 6 independent experiments. Statistical significance: $^{*}p < 0.05$, $^{**}p < 0.01$, and $^{***}p < 0.001$ applicable to all figures.

and [Val^{35}]Aβ42 were statistically significant for monomer and all the oligomers except heptamer (Fig. 1c). The difference between WT Aβ42 and [Nle^{35}]Aβ42 was significant only for dimer, trimer, and hexamer.

Effect of substitution of Met^{35} by Nle or Val on β-sheet formation

We used CD spectroscopy to study the effect of substituting Met^{35} by Nle or Val on conformational changes during Aβ assembly (Fig. 2). In all cases except [Val^{35}]Aβ42, the initial spectrum was characterized by a minimum at 196–200 nm, suggesting that the peptide conformation was pre-dominantly a statistical coil. With incubation, in all cases the minimum at 196–200 nm was replaced by a maximum at 198–199 nm and, in the spectra of Aβ42 analogs, was accompanied by formation of a minimum at 215–217 nm, which is indicative of formation of β-sheet. A similar minimum typically is observed for Aβ40 analogs at higher peptide concentrations (Kirkitadze *et al.* 2001). We chose to keep the concentration consistent across all assays and therefore did not observe the typical minimum at 215 nm for Aβ40 analogs here.

Substitution of Met^{35} by Nle slightly increased, whereas substitution by Val slightly decreased the kinetics of conformational change in Aβ40. The kinetics of conformational transition in [Nle^{35}]Aβ42 was slightly increased relative to WT Aβ42, whereas β-sheet formation by [Val^{35}]Aβ42 was apparent already at the first time point (∼ 5 min after dissolution) and was faster than the kinetics of conformational change in [Nle^{35}]Aβ42 or WT Aβ42 (Fig. 2). These observations correlated with the trends observed in the PICUP experiments, i.e., higher abundance of larger oligomers correlated with faster kinetics of β-sheet formation.

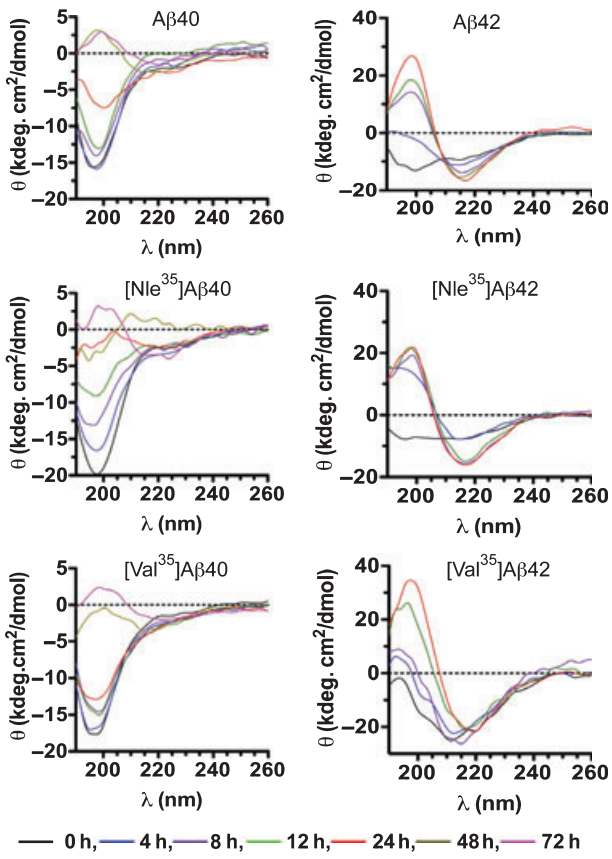

Fig. 2 Conformational change kinetics of amyloid β-protein (Aβ) analogs. Aβ40, Aβ42, and their Nle^{35}- or Val^{35}-substituted analogs were incubated at 25°C with agitation and the solutions monitored periodically by circular dichroism spectroscopy. Aβ40 analogs were measured up to 72 h and Aβ42 analogs up to 24 h. The spectra are representative of three independent experiments.

Effect of substitution of Met^{35} by Nle or Val on assembly size

We used DLS to monitor the initial assembly size distribution of the Aβ analogs and the progressive growth of aggregation size. In our experience, unlike Aβ42, which shows formation of intermediate particle sizes during aggregation, in DLS experiments, Aβ40 initially shows only particles of R_H ∼ 1–2 nm and following incubation (typically ≥ 1 week), very large particles appear, without accumulation of intermediate size particles (Bitan *et al.* 2003a). Based on this experience and because the effect of substitution by Nle or Val on Aβ40 found using PICUP or CD was relatively small, we did no expect DLS experiments with Aβ40 to add useful information and studied only Aβ42 analogs by DLS. We measured both the change in particle size and the frequency of intensity spikes that occur when very large particles cross the laser beam. For aggregating peptides, the frequency of intensity spikes can be used to estimate the rate of fibril formation (Fradinger *et al.* 2008).

Initially the WT and substituted Aβ42 analogs formed pre-dominantly particles of hydrodynamic radius (R_H) = 10–30 nm (Fig. 3) and no intensity spikes. This situation was unchanged after 24 h of incubation and remained stable for several days. After 7 days, the same distribution and no intensity spikes still were observed for WT Aβ42, whereas particles of R_H = 100–200 nm appeared for both substituted analogs, which also displayed occasional intensity spikes, indicating the beginning of fibril formation. By 14 days of incubation, particles of R_H = 100–200 nm were observed also for WT Aβ42. At the same time, particles of R_H = 1000–2000 nm were detected for the two substituted analogs. The faster kinetics of [Nle^{35}]Aβ42 and [Val^{35}]Aβ42 relative to WT Aβ42 correlated with the PICUP and CD data.

It is important to note that because in DLS measurements the intensity is proportional to the square of the mass, the populations of larger particles are highly over-represented in Fig. 3. Particles of R_H = 10–15 nm still existed at all time

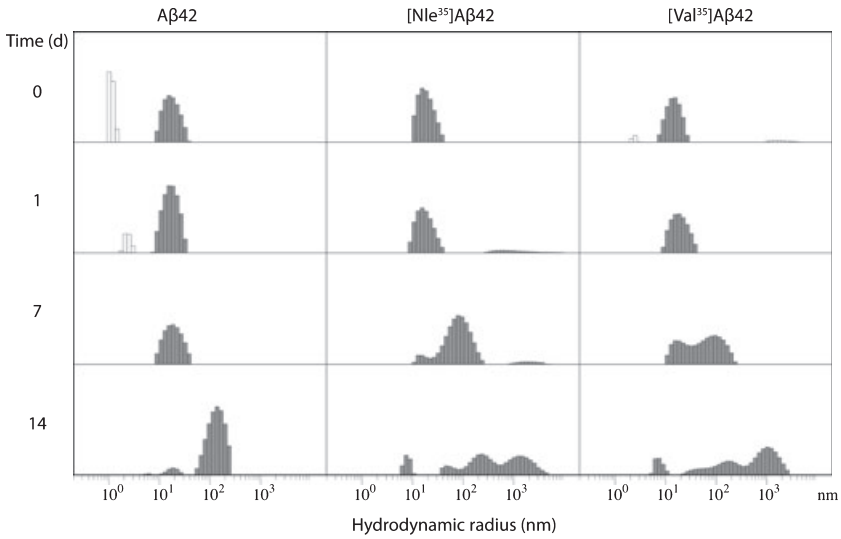

Fig. 3 Particle size growth of amyloid β-protein (Aβ) analogs. Aβ42 and its Nle[35]- or Val[35]-substituted analogs were filtered through a 20-nm pore size filter, incubated at 25°C under quiescent conditions and monitored by dynamic light scattering for up to 14 days.

points in all cases but they were over-shadowed by the intensity of larger particles.

The overall slower kinetics of aggregation in the DLS experiments compared with CD and EM (see below) reflects the different preparation and incubation conditions. Samples measured by DLS must be filtered to remove dust particles and are incubated without agitation. Without these measures, large particles render the measurements useless already at the very early time points.

Effect of substitution of Met[35] by Nle or Val on morphology

The morphology of the WT and substituted peptides was examined by EM immediately after preparation and after 72 h (Aβ40) or 24 h (Aβ42) of incubation (Fig 4). All the peptides initially had non-fibrillar morphology and showed structures consistent with oligomers. Following 72 h of incubation, the morphology of Aβ40 and [Nle[35]]Aβ40 did not change. The behavior of [Val[35]]Aβ40 was less consistent. In some experiments, this peptide showed a mixture of oligomers and fibrils whereas in others, its morphology was similar to Aβ40 and [Nle[35]]Aβ40 (Fig 4). Aβ42 and both its substituted analogs showed abundant fibrils after 24 h of incubation. Quasi-spherical oligomers still could be observed in all cases (Fig 4).

Taken together, the results of most of the biophysical experiments show that substitution of Met by Nle or Val increases the tendency of Aβ to self-assemble. This tendency correlates with the higher hydrophobicity of Nle and Val relative to Met.

Effect of substitution of Met[35] by Nle or Val on Aβ neurotoxicity

To study the structure – activity relationships of substituted Aβ analogs, we treated rat primary cortical or hippocampal neurons with WT, Nle-, or Val-substituted Aβ40 or Aβ42 and measured neurotoxicity using the MTT reduction, LDH release, and TUNEL staining assays. We used these three different assays because each measures a different aspect of cell viability: The MTT assay measures mitochondrial activity of viable cells (Wang *et al.* 2006), the LDH assay signifies membrane integrity and is a direct measurement of cell death (Decker and Lohmann-Matthes 1988), and the TUNEL assay indicates DNA fragmentation and denotes apoptosis.

Because Aβ42 is substantially more toxic than Aβ40, we performed full dose-response analysis (at 1–100 μM) for Aβ42 analogs using both the MTT and LDH assays, whereas the toxicity of Aβ40 analogs was assessed at a single concentration—10 μM, for comparison with Aβ42 analogs and to facilitate correlating the data with the results of the biophysical measurements described above.

Using the MTT assay, the concentrations at which 50% of the maximal toxicity (EC_{50}) was observed were 10 ± 2 μM, 11 ± 3, and 9 ± 1 for Aβ42, [Nle[35]]Aβ42, and [Val[35]]Aβ42, respectively (Fig. 5a). The EC_{50} values measured using the LDH assay were 11 ± 5, 11 ± 5, and 12 ± 8 for Aβ42, [Nle[35]]Aβ42, and [Val[35]]Aβ42, respectively (Fig 5b). Comparison of the neurotoxicity at 10 μM showed that the toxicity of the substituted analogs was similar to that of the WT peptides for both Aβ40 and Aβ42 alloforms using both the MTT (Fig. 5c) and LDH (Fig 5d) assays. In all cases, the only statistically significant differences were found between Aβ42 and Aβ40 analogs, whereas the differences between the substituted analogs and the corresponding WT Aβ alloforms were small and statistically insignificant. Cortical and hippocampal neurons showed similar sensitivity to Aβ analogs in most experiments.

Similar results were obtained using the TUNEL assay, which showed that all the Aβ analogs induced apoptosis.

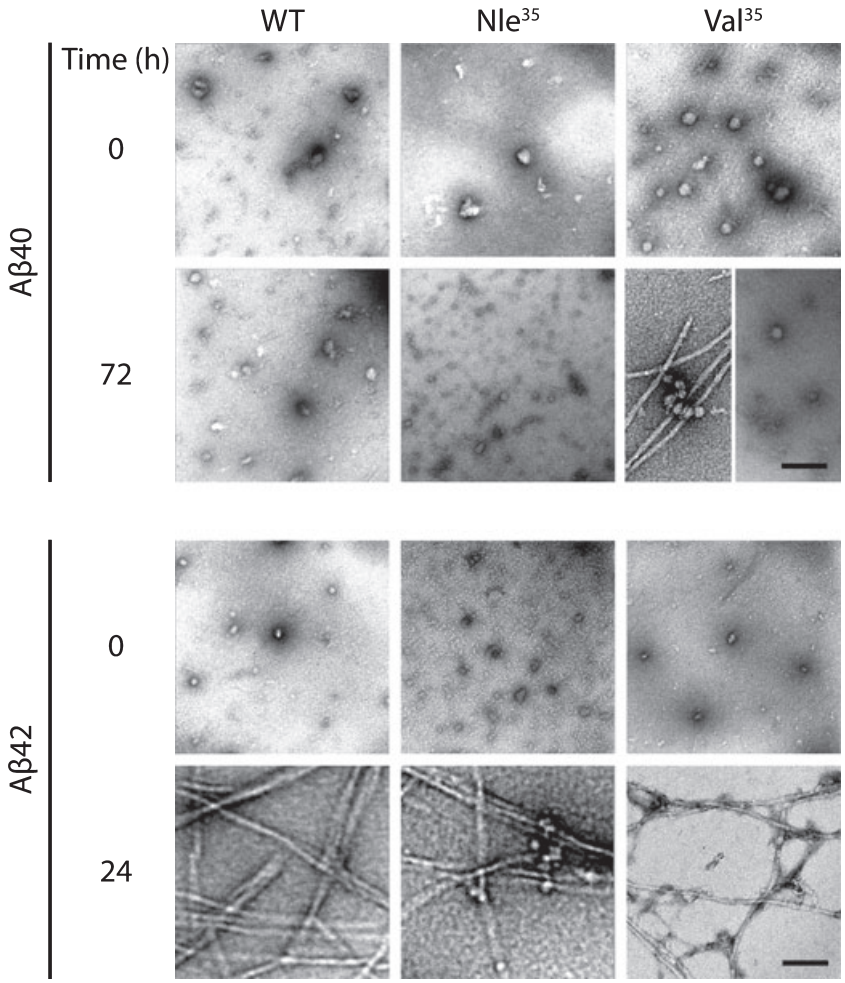

Fig. 4 Time-dependent morphological change in amyloid β-protein (Aβ) analogs. Aβ analogs were incubated at 25°C for 72 h (Aβ40) or 24 h (Aβ42) with agitation. Aliquots were spotted at the beginning and end of the measurement on glow-discharged, carbon-coated grids, stained with uranyl acetate, and examined by EM. The images are representative of three independent experiments. The scale bars indicate 100 nm and are applicable to all images.

Aβ42 analogs were significantly more toxic that Aβ40 analogs yet no significant differences were found between the Nle- or Val-substituted analogs and the WT peptides (Fig 6).

Discussion

Substitution of Met^{35} in Aβ by redox-unreactive, aliphatic groups has been reported to both decrease, in the case of Nle (Varadarajan *et al.* 1999; Butterfield and Boyd-Kimball 2005; Clementi *et al.* 2006; Piacentini *et al.* 2008), and increase, in case of Val (Ciccotosto *et al.* 2004) Aβ neurotoxicity, with no satisfactory explanation for these contradictory observations. The toxicity findings also were not correlated directly with the assembly properties of the substituted analogs. To re-evaluate these data, we compared the Nle- and Val-substituted and WT analogs of both Aβ40 and Aβ42 using multiple biophysical and cytotoxicity assays.

Using four different biophysical assays, we found that substituting Met^{35} by Nle or Val tended to increase Aβ assembly. The substitutions effect on the oligomer size distribution (Fig. 1a) or conformational change kinetics (Fig. 2) of Aβ40 was modest relative to the effect on Aβ42. In particular, substitution of Met^{35} by Val was found to accelerate the aggregation kinetics of Aβ42 (Figs 2 and 3), which correlated with a shift in the oligomer size distribution towards higher order oligomers (Fig. 1a and c). A similar, yet more subtle effect on acceleration of aggregation (Fig. 3) and a shift in oligomer size distribution (Fig. 1c) was observed for [Nle^{35}]Aβ42. Overall, the tendency to increase self-assembly was more pronounced in Aβ42 than in Aβ40 and correlated with the somewhat higher hydrophobicity of Nle and Val relative to Met. These data support a central role for the C-terminus in the assembly of Aβ42 and less so for Aβ40, in agreement with previous reports (Bitan *et al.* 2003a; Urbanc *et al.* 2004; Yun *et al.* 2007; Yang and Teplow 2008; Bernstein *et al.* 2009).

We note that the DLS data obtained for the Aβ42 analogs are comparable qualitatively but not quantitatively with the CD results because of the differences in samples preparation. Using different preparation protocols was necessary because of the fundamental differences between the two methods. Unlike CD, which is an averaging technique, DLS over-emphasizes large particles, as discussed above. Therefore,

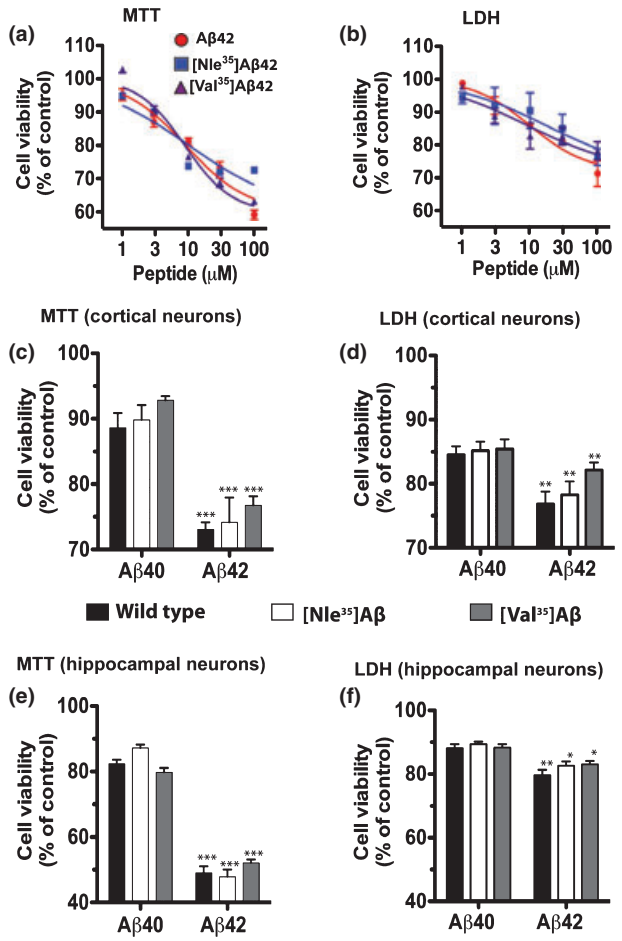

Fig. 5 Amyloid β-protein (Aβ)-induced neurotoxicity measured by the 3-(4,5-dimethylthiazol-2-yl)-2,5-diphenyltetrazolium bromide (MTT) and lactate dehydrogenase (LDH) assays. Rat primary cortical or hippocampal neurons were treated with Aβ40, Aβ42, or their Nle[35]- or Val[35]-substituted analogs for 48 h. Cell viability was assayed by measuring MTT reduction by active cells or by LDH release. (a) Dose–response analysis of Aβ42 analogs by the MTT assay in cortical neuron. (b) Dose–response analysis of Aβ42 analogs by the LDH assay in cortical neurons. (c) Cell viability following treatment with 10 μM of each peptide measured by the MTT assay in cortical neurons. (d) Cell viability following treatment with 10 μM of each peptide measured by the LDH assay in cortical neurons. (e) Cell viability following treatment with 10 μM of each peptide measured by the MTT assay in hippocampal neurons. (f) Cell viability following treatment with 10 μM of each peptide measured by the LDH assay in hippocampal neurons. The data are average of three independent experiments with six data points per condition ($n = 18$). $^{*}p < 0.05$, $^{**}p < 0.01$, and $^{***}p < 0.001$ vs the corresponding Aβ40 analog.

DLS samples must be filtered prior to measurement to exclude dust particles and cannot be agitated because formation of even a few large particles as a result of agitation would lead to skewed results. Nevertheless, the capability of DLS to measure assembly dynamics non-invasively and with high sensitivity provides useful, complementary information to the CD and EM measurements.

The correlation we observed between formation of higher order oligomers and increased β-sheet formation concords with recent data showing a similar correlation in isolated Aβ40 oligomers (Ono *et al.* 2009). These data also are in agreement with the acceleration of β-sheet formation by [Val[35]]Aβ42 compared with WT Aβ42 in the presence of lipid vesicles and Cu^{2+} ions observed by Ciccotosto *et al.* using CD (Ciccotosto *et al.* 2004). Compared with the latter study, our data reveal that the faster conformational transition of the Val-substituted peptide likely results from the substitution itself rather than from presence of vesicles or Cu^{2+} ions.

Whereas Ciccotosto *et al.* (2004) reported that at 5 μM both Aβ42 and [Val[35]]Aβ42 showed non-fibrillar morphology both initially and after 72 h of incubation at 37°C (Ciccotosto *et al.* 2004), we found fibrillar morphology for all three Aβ42 analogs after 24 h of incubation. These morphological variations likely result from the difference in experimental setup. We used 10 μM concentration and incubated the peptides at 25°C with continuous agitation, whereas Ciccotosto *et al.* used 5 μM and incubated at 37°C without agitation.

Despite the differences in assembly kinetics and in contrast to previous reports, we found very similar levels of toxicity for the WT and substituted analogs of both Aβ40 and Aβ42 using three different assays, MTT, LDH, and TUNEL, in both cortical and hippocampal primary neurons.

Dose-response analysis for Aβ42 and its analogs showed nearly identical values in both the MTT and LDH assays (Fig. 5). When the toxicity of Aβ40 and Aβ42 analogs measured by all three assays was compared at 10 μM, the same concentration used in the biophysical studies, the only significant difference found was between the Aβ40 and Aβ42 groups, but not among the WT and substituted analogs within each group (Figs 5 and 6).

Differences in experimental settings likely explain the difference between our data and those reported by other groups. One obvious possibility is the source of the peptides used. However, in our experience, the differences in biophysical and biologic behavior between Aβ analogs prepared by the UCLA Biopolymers Laboratory and those from commercial sources are not bigger than typical batch-to-batch variation. Moreover the toxicity of WT Aβ in our study was comparable that observed by the other laboratories (Varadarajan *et al.* 1999; Yatin *et al.* 1999; Ciccotosto *et al.* 2004), suggesting that the peptide source did not contribute significantly to the observed results.

More likely explanations include differences in the peptide preparation methods and cell types used. For example, Varadarajan *et al.* used [Nle[35]]Aβ40 that was pre-incubated for 24 h before addition to culture and measured the effect of this peptide after 6 h of incubation with cells (Varadarajan

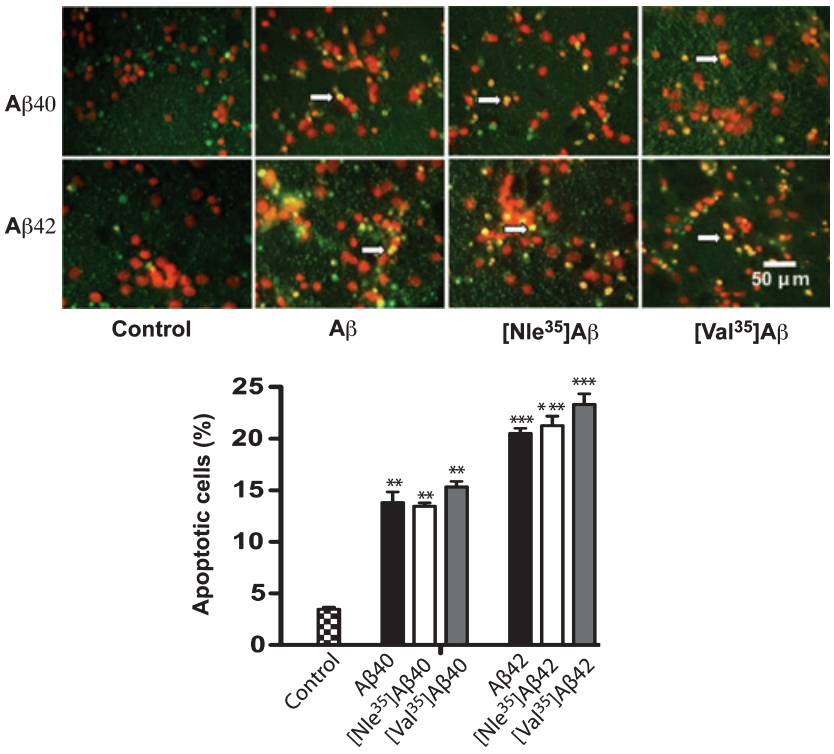

Fig. 6 Amyloid β-protein (Aβ)-induced neuronal apoptosis. Rat primary cortical neurons were grown for 6 days on poly-D-lysine-coated cover slips and then treated with 10 μM of each Aβ analog for 48 h. DNA fragmentation was probed using APO-BrdU staining. Micrographs are representative of 10–15 different fields of each experiment. Arrows indicate terminal deoxyribonucleotidyl transferase dUTP nick end labeling-positive cells. The number of apoptotic cells divided by the total number of cells (counted manually) is expressed as percentage apoptotic death. The data are representative of three independent experiments. $^{**}p < 0.01$ and $^{***}p < 0.001$ versus control.

et al. 1999). Similarly, Yatin *et al.*, used [Nle^{35}]Aβ42, which was dissolved in water at 1 mg/mL, and incubated for 24 h before addition to cells (Yatin *et al.* 1999). In neither case were the peptides treated to remove aggregates prior to their dissolution. In contrast, we treated all the peptides with HFIP to obtain aggregate-free starting conditions, prepared solutions in cell culture media, and added these solutions to the cells immediately after preparation. It is therefore plausible that we observed toxicity of [Nle^{35}]Aβ oligomers, which likely were not present in the former studies because of the 24 h pre-incubation step.

In different studies, Clementi *et al.* (Clementi *et al.* 2006) and Piacentini *et al.* (Piacentini *et al.* 2008) found little or no toxicity for [Nle^{35}]Aβ42 using IMR-32 cells. Though neither group used a pre-incubation step, they diluted the peptides from stock solutions prepared in dimethylsulfoxide directly into the cell culture medium. Thus, the differences between their results and the ones presented here may stem both from the higher sensitivity of primary neurons to Aβ-induced toxicity relative to IMR-32 cells and from the differences in the preparation protocols used.

The higher toxicity of [Val^{35}]Aβ42 relative to WT Aβ42 reported by Ciccotosto *et al.* (Ciccotosto *et al.* 2004), which we did not observe, also may be because of differences in experimental protocols. They prepared their peptides without HFIP treatment and adjusted the concentration based on measurement of absorbance at 214 nm, a method we found to produce results that are inconsistent with amino acid analysis data (G. Bitan, unpublished).

Ciccotosto *et al.* suggested that [Val^{35}]Aβ42 has higher affinity for lipid membranes than Aβ42, which may be linked to increased toxicity, although both Aβ42 and [Val^{35}]Aβ42 were reported to produce similar amount of H_2O_2 (Ciccotosto *et al.* 2004). A different view was suggested by Murray *et al.*, who found that substitution of Met^{35} by Val decreased lipid peroxidation (Murray *et al.* 2005). Because we did not study lipid peroxidation, our data are not directly comparable with those of Murray *et al.* Nevertheless, our results suggest that the presence of Met^{35} in Aβ is not an important factor in Aβ-induced toxicity.

Our conclusion is consistent with a recent elegant study by Butterfield *et al.* (Butterfield *et al.* 2009) who used a variant of the V717F amyloid β-protein precursor transgenic mouse model of AD (Masliah *et al.* 1996), containing an M631L mutation in the amyloid β-protein precursor-encoding gene, which leads to substitution of Met^{35} in Aβ by Leu. The study showed that Met^{35} was required for observation of markers of oxidative stress, such as protein carbonylation and lipid peroxidation in the brains of the mice, yet the substitution of Met^{35} by Leu had no effect on the learning and memory impairment of the mice assessed using the Morris Water Maze (Butterfield *et al.* 2009). The reasons for this apparent discrepancy are not understood and may be related to differences in deposition patterns between WT and [Leu^{35}]Aβ or to involvement of toxic amyloid β-protein precursor fragments other than Aβ, as suggested by the authors (Butterfield *et al.* 2009). As is the case with most mouse models of AD, the impairment of learning and

memory observed by Butterfield *et al.* was not associated with neuronal loss (Morrissette *et al.* 2009). Nonetheless, if one accepts the assumption that the results of the learning and memory tests measured *in vivo* correlate with our neurotoxicity measurements in primary cultures, these results support our conclusion that the presence of Met^{35} is not important for Aβ toxicity.

Acknowledgments

This work was supported by Alzheimer's Association Grant IIRG-07-5833 (GB) and NIH/NIA grant AG027818 (GB and GBB). We thank Margaret M. Condron for peptide synthesis and amino acid analysis, Dr. David Teplow for the use of his CD spectrometer, and Drs. Farid Rahimi and Huiyuan Li for valuable advice and critical discussion of the manuscript.

References

Barnham K. J., Ciccotosto G. D., Tickler A. K. *et al.* (2003) Neurotoxic, redox-competent Alzheimer's β-amyloid is released from lipid membrane by methionine oxidation. *J. Biol. Chem.* **278**, 42959–42965.

Bernstein S. L., Dupuis N. F., Lazo N. D. *et al.* (2009) Amyloid-β protein oligomerization and the importance of tetramers and dodecamers in the aetiology of Alzheimer's disease. *Nat. Chem.* **1**, 326–331.

Bitan G. (2006) Structural study of metastable amyloidogenic protein oligomers by photo-induced cross-linking of unmodified proteins. *Methods Enzymol.* **413**, 217–236.

Bitan G., Lomakin A. and Teplow D. B. (2001) Amyloid β-protein oligomerization: prenucleation interactions revealed by photo-induced cross-linking of unmodified proteins. *J. Biol. Chem.* **276**, 35176–35184.

Bitan G., Kirkitadze M. D., Lomakin A., Vollers S. S., Benedek G. B. and Teplow D. B. (2003a) Amyloid β-protein (Aβ) assembly: Aβ40 and Aβ42 oligomerize through distinct pathways. *Proc. Natl Acad. Sci. USA* **100**, 330–335.

Bitan G., Tarus B., Vollers S. S., Lashuel H. A., Condron M. M., Straub J. E. and Teplow D. B. (2003b) A molecular switch in amyloid assembly: Met^{35} and amyloid β-protein oligomerization. *J. Am. Chem. Soc.* **125**, 15359–15365.

Bitan G., Vollers S. S. and Teplow D. B. (2003c) Elucidation of primary structure elements controlling early amyloid β-protein oligomerization. *J. Biol. Chem.* **278**, 34882–34889.

Bravo R., Arimon M., Valle-Delgado J. J., Garcia R., Durany N., Castel S., Cruz M., Ventura S. and Fernandez-Busquets X. (2008) Sulfated polysaccharides promote the assembly of amyloid β(1-42) peptide into stable fibrils of reduced cytotoxicity. *J. Biol. Chem.* **283**, 32471–32483.

Butterfield D. A. (2002) Amyloid β-peptide (1-42)-induced oxidative stress and neurotoxicity: implications for neurodegeneration in Alzheimer's disease brain. *Free Radic. Res.* **36**, 1307–1313.

Butterfield D. A. and Boyd-Kimball D. (2005) The critical role of methionine 35 in Alzheimer's amyloid β-peptide (1-42)-induced oxidative stress and neurotoxicity. *Biochim. Biophys. Acta* **1703**, 149–156.

Butterfield D. A. and Kanski J. (2002) Methionine residue 35 is critical for the oxidative stress and neurotoxic properties of Alzheimer's amyloid β-peptide 1-42. *Peptides* **23**, 1299–1309.

Butterfield D. A., Reed T., Newman S. F. and Sultana R. (2007) Roles of amyloid β-peptide-associated oxidative stress and brain protein modifications in the pathogenesis of Alzheimer's disease and mild cognitive impairment. *Free Radic. Biol. Med.* **43**, 658–677.

Butterfield D. A., Galvan V., Lange M. B. *et al.* (2009) In vivo oxidative stress in brain of Alzheimer disease transgenic mice: requirement for methionine 35 in amyloid β-peptide of APP. *Free Radic. Biol. Med.* **48**, 136–144.

Ciccotosto G. D., Tew D., Curtain C. C. *et al.* (2004) Enhanced toxicity and cellular binding of a modified amyloid β peptide with a methionine to valine substitution. *J. Biol. Chem.* **279**, 42528–42534.

Clementi M. E., Pezzotti M., Orsini F., Sampaolese B., Mezzogori D., Grassi C., Giardina B. and Misiti F. (2006) Alzheimer's amyloid β-peptide (1-42) induces cell death in human neuroblastoma via bax/bcl-2 ratio increase: an intriguing role for methionine 35. *Biochem. Biophys. Res. Commun.* **342**, 206–213.

Crouch P. J., Harding S. M., White A. R., Camakaris J., Bush A. I. and Masters C. L. (2008) Mechanisms of Aβ mediated neurodegeneration in Alzheimer's disease. *Int. J. Biochem. Cell Biol.* **40**, 181–198.

Cummings J. L. (2004) Alzheimer's disease. *N. Engl. J. Med.* **351**, 56–67.

Dahlgren K. N., Manelli A. M., Stine Jr W. B., Baker L. K., Krafft G. A. and LaDu M. J. (2002) Oligomeric and fibrillar species of amyloid-β peptides differentially affect neuronal viability. *J. Biol. Chem.* **277**, 32046–32053.

Decker T. and Lohmann-Matthes M. L. (1988) A quick and simple method for the quantitation of lactate dehydrogenase release in measurements of cellular cytotoxicity and tumor necrosis factor (TNF) activity. *J. Immunol. Methods* **115**, 61–69.

Fancy D. A. and Kodadek T. (1999) Chemistry for the analysis of protein-protein interactions: rapid and efficient cross-linking triggered by long wavelength light. *Proc. Natl Acad. Sci. USA* **96**, 6020–6024.

Fradinger E. A., Monien B. H., Urbanc B. *et al.* (2008) C-terminal peptides coassemble into Aβ42 oligomers and protect neurons against Aβ42-induced neurotoxicity. *Proc. Natl Acad. Sci. USA* **105**, 14175–14180.

Haass C. and Selkoe D. J. (2007) Soluble protein oligomers in neurodegeneration: lessons from the Alzheimer's amyloid β-peptide. *Nat. Rev. Mol. Cell Biol.* **8**, 101–112.

Halliwell B. (1989) Free radicals, reactive oxygen species and human disease: a critical evaluation with special reference to atherosclerosis. *Br. J. Exp. Pathol.* **70**, 737–757.

Halliwell B. (2006) Oxidative stress and neurodegeneration: where are we now? *J. Neurochem.* **97**, 1634–1658.

Hardy J. and Selkoe D. J. (2002) The amyloid hypothesis of Alzheimer's disease: progress and problems on the road to therapeutics. *Science* **297**, 353–356.

Hou L., Kang I., Marchant R. E. and Zagorski M. G. (2002) Methionine 35 oxidation reduces fibril assembly of the amyloid Aβ-(1-42) peptide of Alzheimer's disease. *J. Biol. Chem.* **277**, 40173–40176.

Hou L., Shao H., Zhang Y. *et al.* (2004) Solution NMR studies of the Aβ(1-40) and Aβ(1-42) peptides establish that the Met35 oxidation state affects the mechanism of amyloid formation. *J. Am. Chem. Soc.* **126**, 1992–2005.

Jarrett J. T., Berger E. P. and Lansbury Jr P. T. (1993) The carboxy terminus of the β amyloid protein is critical for the seeding of amyloid formation: implications for the pathogenesis of Alzheimer's disease. *Biochemistry* **32**, 4693–4697.

Josephs K. A., Whitwell J. L., Ahmed Z. *et al.* (2008) β-Amyloid burden is not associated with rates of brain atrophy. *Ann. Neurol.* **63**, 204–212.

Kirkitadze M. D., Condron M. M. and Teplow D. B. (2001) Identification and characterization of key kinetic intermediates in amyloid β-protein fibrillogenesis. *J. Mol. Biol.* **312**, 1103–1119.

Koffie R. M., Meyer-Luehmann M., Hashimoto T. *et al.* (2009) Oligomeric amyloid β associates with postsynaptic densities and correlates with excitatory synapse loss near senile plaques. *Proc. Natl Acad. Sci. USA* **106**, 4012–4017.

Kuo Y. M., Kokjohn T. A., Beach T. G. *et al.* (2001) Comparative analysis of amyloid-β chemical structure and amyloid plaque morphology of transgenic mouse and Alzheimer's disease brains. *J. Biol. Chem.* **276**, 12991–12998.

Lomakin A., Chung D. S., Benedek G. B., Kirschner D. A. and Teplow D. B. (1996) On the nucleation and growth of amyloid β-protein fibrils: detection of nuclei and quantitation of rate constants. *Proc. Natl Acad. Sci. USA* **93**, 1125–1129.

Markesbery W. R. and Lovell M. A. (1998) Four-hydroxynonenal, a product of lipid peroxidation, is increased in the brain in alzheimers-disease. *Neurobiol. Aging* **19**, 33–36.

Masliah E., Sisk A., Mallory M., Mucke L., Schenk D. and Games D. (1996) Comparison of neurodegenerative pathology in transgenic mice overexpressing V717F β-amyloid precursor protein and Alzheimer's disease. *J. Neurosci.* **16**, 5795–5811.

Morrissette D. A., Parachikova A., Green K. N. and LaFerla F. M. (2009) Relevance of transgenic mouse models to human Alzheimer disease. *J. Biol. Chem.* **284**, 6033–6037.

Murray I. V., Sindoni M. E. and Axelsen P. H. (2005) Promotion of oxidative lipid membrane damage by amyloid β proteins. *Biochemistry* **44**, 12606–12613.

Näslund J., Schierhorn A., Hellman U. *et al.* (1994) Relative abundance of Alzheimer Aβ amyloid peptide variants in Alzheimer disease and normal aging. *Proc. Natl Acad. Sci. USA* **91**, 8378–8382.

Ono K., Condron M. M. and Teplow D. B. (2009) Structure-neurotoxicity relationships of amyloid β-protein oligomers. *Proc. Natl Acad. Sci. USA* **106**, 14745–14750.

Palmblad M., Westlind-Danielsson A. and Bergquist J. (2002) Oxidation of methionine 35 attenuates formation of amyloid β -peptide 1-40 oligomers. *J. Biol. Chem.* **277**, 19506–19510.

Piacentini R., Ripoli C., Leone L., Misiti F., Clementi M. E., D'Ascenzo M., Giardina B., Azzena G. B. and Grassi C. (2008) Role of methionine 35 in the intracellular Ca^{2+} homeostasis dysregulation and Ca^{2+}-dependent apoptosis induced by amyloid β-peptide in human neuroblastoma IMR32 cells. *J. Neurochem.* **107**, 1070–1082.

Rahimi F., Maiti P. and Bitan G. (2009) Photo-induced cross-linking of unmodified proteins (PICUP) applied to amyloidogenic peptides. *J. Vis. Exp.* DOI: 10.3791/1071.

Reiman E. M., Chen K., Liu X. *et al.* (2009) Fibrillar amyloid-β burden in cognitively normal people at 3 levels of genetic risk for Alzheimer's disease. *Proc. Natl Acad. Sci. USA* **106**, 6820–6825.

Roher A. E., Palmer K. C., Yurewicz E. C., Ball M. J. and Greenberg B. D. (1993) Morphological and biochemical analyses of amyloid plaque core proteins purified from Alzheimer disease brain tissue. *J. Neurochem.* **61**, 1916–1926.

Roychaudhuri R., Yang M., Hoshi M. M. and Teplow D. B. (2009) Amyloid β-protein assembly and Alzheimer disease. *J. Biol. Chem.* **284**, 4749–4753.

Segal M. and Manor D. (1992) Confocal microscopic imaging of $[Ca^{2+}]_i$ in cultured rat hippocampal neurons following exposure to *N*-methyl-D-aspartate. *J. Physiol.* **448**, 655–676.

Selkoe D. J. (2001) Alzheimer's disease: genes, proteins, and therapy. *Physiol. Rev.* **81**, 741–766.

Tomic J. L., Pensalfini A., Head E. and Glabe C. G. (2009) Soluble fibrillar oligomer levels are elevated in Alzheimer's disease brain and correlate with cognitive dysfunction. *Neurobiol. Dis.* **35**, 352–358.

Urbanc B., Cruz L., Yun S., Buldyrev S. V., Bitan G., Teplow D. B. and Stanley H. E. (2004) *In silico* study of amyloid β-protein folding and oligomerization. *Proc. Natl Acad. Sci. USA* **101**, 17345–17350.

Varadarajan S., Yatin S., Kanski J., Jahanshahi F. and Butterfield D. A. (1999) Methionine residue 35 is important in amyloid β-peptide-associated free radical oxidative stress. *Brain Res. Bull.* **50**, 133–141.

Varadarajan S., Yatin S., Aksenova M. and Butterfield D. A. (2000) Review: Alzheimer's amyloid β-peptide-associated free radical oxidative stress and neurotoxicity. *J. Struct. Biol.* **130**, 184–208.

Varadarajan S., Kanski J., Aksenova M., Lauderback C. and Butterfield D. A. (2001) Different mechanisms of oxidative stress and neurotoxicity for Alzheimer's Aβ(1-42) and Aβ(25-35). *J. Am. Chem. Soc.* **123**, 5625–5631.

Vollers S. S., Teplow D. B. and Bitan G. (2005) Determination of peptide oligomerization state using rapid photochemical crosslinking. *Methods Mol. Biol.* **299**, 11–18.

Wang X., Ge J., Wang K., Qian J. and Zou Y. (2006) Evaluation of MTT assay for measurement of emodin-induced cytotoxicity. *Assay Drug Dev. Technol.* **4**, 203–207.

White J. A., Manelli A. M., Holmberg K. H., Van Eldik L. J. and LaDu M. J. (2005) Differential effects of oligomeric and fibrillar amyloid-β 1-42 on astrocyte-mediated inflammation. *Neurobiol. Dis.* **18**, 459–465.

Yang M. and Teplow D. B. (2008) Amyloid β-protein monomer folding: free-energy surfaces reveal alloform-specific differences. *J. Mol. Biol.* **384**, 450–464.

Yatin S. M., Varadarajan S., Link C. D. and Butterfield D. A. (1999) In vitro and in vivo oxidative stress associated with Alzheimer's amyloid β-peptide (1-42). *Neurobiol. Aging* **20**, 325–330.

Yun S., Urbanc B., Cruz L., Bitan G., Teplow D. B. and Stanley H. E. (2007) Role of electrostatic interactions in amyloid β-protein (Aβ) oligomer formation: a discrete molecular dynamics study. *Biophys. J.* **92**, 4064–4077.

